Tellus (2007), 59A, 170–181
Printed in Singapore. All rights reserved

TELLUS

How useful are teleconnection patterns for explaining variability in extratropical storminess?

By I. A. SEIERSTAD[1,2]*, D. B. STEPHENSON[2,3] and N. G. KVAMSTØ[1,2], [1]*Geophysical Institute, University of Bergen, Norway;* [2]*Bjerknes Centre for Climate Research, Bergen, Norway;* [3]*Department of Meteorology, The University of Reading, Reading, United Kingdom*

(Manuscript received 23 June 2006; in final form 11 December 2006)

ABSTRACT

This empirical study relates the extratropical storminess in the Northern Hemisphere to the large-scale flow using gamma regression models. Time series of storminess are derived using the monthly mean variance of highpass filtered sea-level pressure from the 6-hourly NCEP/NCAR reanalysis data for the 54 extended winters (Oct-Mar) between 1950–2003. Five teleconnection patterns were found to be statistically significant factors at the 5% level for storminess in the Euro-Atlantic region: the North Atlantic Oscillation (NAO), the East Atlantic pattern, the Scandinavian pattern, the East-Atlantic/Western-Russia pattern and the Polar/Eurasian pattern. In the North Pacific the dominant factor is found to be the Pacific North American (PNA) pattern. It is also shown that the relationship between teleconnection patterns and storminess to a large extent is accounted for by a basic relation between storminess and the local mean SLP but with a few notable exceptions. In particular the East Atlantic pattern is identified as an important non-local factor for storminess over the Labrador Sea and the PNA pattern as an important non-local factor for storminess north of the Aleutian low.

1. Introduction

During the last decade there has been an emphasis on the North Atlantic Oscillation (NAO) and the Pacific North American (PNA) pattern as the leading large-scale patterns in the Northern Hemisphere for representing climate variability. In particular, Quadrelli and Wallace (2004) have argued the prominence of the NAO and PNA partly on the basis of how much of the total hemispheric variance of sea-level pressure (SLP) they account for. The explained fraction of the total variance increases substantially from monthly to seasonal and longer timescales suggesting that these two patterns are a sufficient basis for studying climate variability in the extratropics on these timescales.

In this paper a different approach is used in order to assess the relevance of teleconnection patterns. Rather than focusing on how much of the total variance of the SLP field they explain we will investigate to what extent teleconnection patterns account for wintertime synoptic activity in the extratropics. Recently Mailier et al. (2006) have shown that as many as five teleconnection patterns are important factors for the variability of cyclone counts in the North Atlantic and over western Europe. To relate the mean flow to synoptic activity is potentially very useful for time periods when observations are too few to reliably represent synoptic activity. Chang and Fu (2003), for instance, have used changes in the mean flow field to describe interdecadal storm track variability for the first part of the 20th century.

Synoptic activity in the extratropics has for a long time been discussed with reference to a mean flow. For instance, Pettersen (1956) observed that cyclones in the North Atlantic tend to travel northeastward and merge with the background subpolar low and Rex (1950) observed that cyclones tend to move round high pressure anomalies. Although any separation of the flow into synoptic activity and low-frequency flow (here a timescale of about 10–90 d) is somewhat arbitrary the distinction has proved highly useful. Wallace et al. (1988) showed that many of the characteristics of highpass filtered geopotential height fields are relatively insensitive to the applied filter provided disturbances in the band from 2.5–6 d are retained. Such disturbances resemble zonally orientated wave trains with a mean wavelength of 4000 km, tilting westward with height and steered by the 700 hPa flow (Blackmon et al., 1984a,b). Such waves, therefore, share many of the characteristics with synoptic scale baroclinic waves (i.e. Holton, 1992). An extensive review of the literature on extratropical storm tracks defined using temporal highpass filters can be found in Chang et al. (2002).

The origin of extratropical intraseasonal variability is less well defined. As pointed out by Vallis et al. (2004), the equivalent barotropic structure of the low-frequency patterns found near

*Corresponding author.
e-mail: ivar@gfi.uib.no
DOI: 10.1111/j.1600-0870.2007.00226.x

the middle and end of the major storm tracks suggests a synoptic origin for these. They showed that the spatial structure of the North Atlantic Oscillation can be simulated by a non-divergent barotropic model with a stochastic forcing representing the fluctuating forcing of baroclinic waves. The reddening of the power spectrum of the NAO in their model is simply caused by friction and the non-linear dynamics of the model and not external factors such as SST anomalies. The important role for synoptic eddies in producing low-frequency variability is also consistent with numerous observational studies. The forcing due to high-frequency fluxes of vorticity and heat has been shown to be strongly related to local low-frequency geopotential height tendencies (Lau and Holopainen, 1984; Lau, 1988; Lau and Nath, 1991). Furthermore, Lau (1988) also showed that the leading modes describing the variability in the position of the storm tracks have a strong linear relationship to the monthly mean flow in the middle troposphere. On the modelling side, Whitaker and Sardeshmukh (1998) managed to reproduce many aspects of extratropical synoptic eddy statistics using a quasi-geostrophic model linearized about the long-term mean flow with a white Gaussian forcing.

Based on earlier observational and modelling studies it is thus reasonable to expect that a measure of local synoptic activity and local low-frequency variability in the extratropics to some extent have a linear relationship. A natural question then is whether teleconnection patterns can provide any additional explanation for storminess. One might expect this given that some teleconnection patterns, like the PNA and the Scandinavian pattern are often viewed as a Rossby wave response to tropical convection anomalies (Hoskins and Karoly, 1981; Trenberth et al., 1998). In such a view the extratropical low-frequency variability is largely due to tropical forcing with associated changes in the major jet streams and extratropical storminess. Alternatively, we may hypothesize that the linear relationship between teleconnection patterns and storminess is primarily reflected by a relationship between the local mean flow and storminess. In consequence, teleconnection patterns with a centre of variability near the major storm tracks will be linearly related to storminess due to this basic relationship. In order to test this simple hypothesis we will in this study, therefore, address the following questions in a linear perspective:

(i) How well can variations in local mean flow account for variations in extratropical storminess?

(ii) To what extent can non-local mean flow (i.e. teleconnection patterns) provide additional explanation for variations in storminess?

(iii) How much of the variability of storminess can be accounted for by the NAO and PNA patterns? Are other teleconnection patterns important for predicting storminess in the Euro-Atlantic region and in the North Pacific?

These questions will be answered within a regression framework where the relative importance of different factors can be assessed. For this purpose we are using generalized linear models (GLMs). Such models have in particular been useful for modelling daily precipitation (Coe and Stern, 1982; Sapiano et al., 2006). Other applications have included modelling of maximum daily wind speed (Yan et al., 2002) and Poisson regression of storm counts (Paciorek et al., 2002; Elsner and Bossak, 2003; Mailier et al., 2006). A review of applications for GLMs in climate science is provided by Chandler (2005).

The paper will proceed as follows. Section 2 provides a description of the meteorological data used together with a description of how measures of storminess and teleconnection patterns are defined. The modelling strategy for answering the questions posed in the introduction is also presented in Section 2. The results from the generalized linear models are shown in Section 3. Finally, in Section 4 the main findings are summarized and discussed.

2. Data and methodology

2.1. Storminess

This study is using the SLP field from the reanalysis by the National Centers for Environmental Prediction—National Center for Atmospheric Research (NCEP/NCAR) (Kalnay et al., 1996). It is the longest reanalysis data set available at 6-hr resolution and 54 extended winters (October to March 1950–2003) are studied. Extended winters are chosen in order to show the relevance of less known teleconnection patterns such as the Scandinavian Pattern which is known to be particularly active during the transition seasons from autumn to winter and winter to spring.

A measure of monthly storminess Y is derived using the following procedure:

(i) SLP anomalies for every 6 hr were created by subtracting the 54 yr long term mean for the corresponding day.

(ii) Lowpass filtered anomalies were then obtained by applying a 61 point 10-d lowpass filter as described in Doblas-Reyes and Déqué (1998). The filter weights are shown in Table 1 for reference. The highpass filtered $\mathrm{SLP}^{\mathrm{high}}$ were found by subtracting the lowpass filtered SLP from the original anomalies

(iii) Monthly mean values of the variance of the highpass filtered SLP were then calculated as: $Y = \frac{1}{120}\sum_{i=1}^{120}(\mathrm{SLP}_i^{\mathrm{high}})^2$ giving 324 monthly values of storminess.

The SLP field is chosen because it is known to be well constrained by observations in the reanalysis data (Chang and Fu, 2003). A possible drawback is that this field is dominated by large spatial scales so that small-scale features, such as storms in the Mediterranean, will not be as well captured by highpass filtered SLP compared to for instance relative vorticity. Note that synoptic storm tracks, as defined by tracking minima in SLP, are in general not identical to maxima in the variance of highpass filtered SLP (Hoskins and Hodges, 2002). The latter are more zonal since they do not discriminate between cyclones and anticyclones. Despite this such variance maxima are in the literature

Table 1. Filter weights for the 61 point 10-d lowpass filter given by: $Y_t = \sum_{k=-30}^{30} w_k X_{t+k}$. The filter is symmetric (i.e., $w_k = w_{-k}$)

k	w_k	k	w_k
0	−0.0001768	16	0.0126500
1	−0.0005586	17	0.0158571
2	−0.0009547	18	0.0192771
3	−0.0013324	19	0.0228465
4	−0.0016536	20	0.0264936
5	−0.0018764	21	0.0301396
6	−0.0019571	22	0.0337019
7	−0.0018510	23	0.0370962
8	−0.0015151	24	0.0402392
9	−0.0009095	25	0.0430520
10	0.0000000	26	0.0454623
11	0.0012405	27	0.0474069
12	0.0028299	28	0.0488345
13	0.0047759	29	0.0497066
14	0.0070743	30	0.0500000
15	0.0097086		

referred to as *storm tracks*. The results presented in this study are not very sensitive to the chosen filter. A simple 8-d running mean filter gives qualitatively similar results (not shown).

2.2. Teleconnection patterns

The teleconnection indices are obtained from the Climate Prediction Center (CPC). The CPC has recently (1 July 2005) revised its calculation of the ten leading Northern Hemisphere teleconnection indices which can be downloaded from the CPC website (www.cpc.noaa.gov). A list of these are shown in Table 2. The Pacific Transition Pattern is not included since it is only active during summer. The Northern Hemisphere teleconnection patterns and corresponding indices are calculated using Rotated Principal Component Analysis (RPCA) (Barnston and Livezey, 1987). The RPCA procedure was applied to standardized monthly mean 500 hPa height anomalies in the region 20^0N-90^0N between January 1950 and December 2000. The indices have been standardized to zero mean and unit variance and their value is set to zero for the months were the patterns are inactive. A review of these teleconnection patterns is provided by Panagiotopoulos et al. (2002).

Table 2. The CPC Northern Hemisphere teleconnection indices. The right column showing the months when the patterns are not active. The monthly indices can be obtained from the CPC website (www.cpc.noaa.gov)

i	Teleconnection pattern	$y_i = 0$
1	North Atlantic Oscillation	
2	East Atlantic Pattern	
3	West Pacific Pattern	
4	East Pacific/North Pacific Pattern	December
5	Pacific North American Pattern	
6	East Atlantic/West Russia Pattern	
7	Scandinavian Pattern	
8	Tropical Northern Hemisphere Pattern	October, November, March
9	Polar Eurasia Pattern	

2.3. Gamma regression models for storminess

Generalized linear models provide a regression framework where a probability distribution and a relationship between the mean and the variance need to be specified. Since variance of highpass filtered SLP is a positively valued variable a natural candidate is the Gamma probability distribution. The great advantage of using the Gamma probability distribution is its flexibility for modelling positively valued distributions of many different shapes. A property that is particularly useful since the probability distribution of storminess differ in shape along the major storm tracks, as will be shown later in Fig. 8. The parameters of the Gamma distribution are the mean μ and the shape parameter ν. Both parameters need to be estimated but the shape parameter is assumed constant for all observations at a grid point. For further details about the Gamma distribution see the Appendix A1.

In a GLM the expected value μ is related to a linear predictor using a *link* function. For the Gamma distribution it is convenient to use the *log* link to ensure that all fitted values are positive. The monthly storminess Y at a grid point can then be related to the large-scale flow using the following GLM:

$$Y|\eta \sim Gamma(\mu, \nu)$$

$$\nu = constant$$

$$ln(\mu) = \eta = \alpha_0 + \sum_{i=1}^{5} \alpha_i x_i + \sum_{j=1}^{p} \beta_j y_j + \beta t, \quad (1)$$

where the first line states that the monthly storminess Y, conditional on a linear predictor η, is Gamma distributed. In a GLM we are thus predicting a probability distribution for Y given a value of the predictor. The regression coefficients α and β are estimated by maximum likelihood calculated by the MATLAB function *glmfit*. This function uses an iterative weighted least-squares algorithm described in McCullagh and Nelder (1989). Following Mailier et al. (2006), seasonality is accounted for by including five binary indicator variables x_i for November to March. A sixth indicator for October is redundant because its state (0 or 1) is fully determined by the states of the other five indicator variables. The estimated mean storminess for October is then given by e^{α_0}, the November mean by $e^{\alpha_0+\alpha_1}$, the December mean by $e^{\alpha_0+\alpha_2}$ and so on. The predictor variables y_j in eq. (1) are the local SLP anomaly and the nine leading CPC teleconnection indices. Each of the regression coefficients β_j is then a measure of how the logarithm of mean storminess depends on the predictor

variables y_j. The model is thus multiplicative where $(e^{\beta j} - 1) \times 100$ measures the percentage change in mean storminess for a change of one standard deviation in the predictor.

As seen from eq. (1) an annual linear trend term t, with numbers from 1 to 54 representing the year, was also tested as the last predictor. However, this factor was not significant at the 5 % level in the extratropics when the other factors were accounted for. It is, therefore, not included in the models presented here. To estimate long-term trends in storminess based on reanalysis data is a contentious issue due to the changes in the observational network and the relatively short available time-series with high interannual variability. Harnik and Chang (2003) provide a discussion of this issue and show that the trend in storminess based on rawinsonde observations is substantially smaller than that implied by the reanalysis data.

In order to address the questions posed in the introduction the following five models are fitted to the monthly storminess data:

(i) A model with just a constant term

(ii) A seasonal model including only seasonal factors as predictors

(iii) A local model including seasonal factors and the local SLP anomaly as predictors.

(iv) A teleconnection model including seasonal factors and the nine leading CPC teleconnections as predictors.

(v) A full model including seasonal factors, the local SLP anomaly and all the teleconnection indices as predictors.

The statistical significance of the factors are calculated using likelihood ratio tests. As pointed out by Yan et al. (2002) such tests are particularly useful for identifying weak signals in noisy data. The procedure for such hypothesis testing is shown in the Appendix A2.

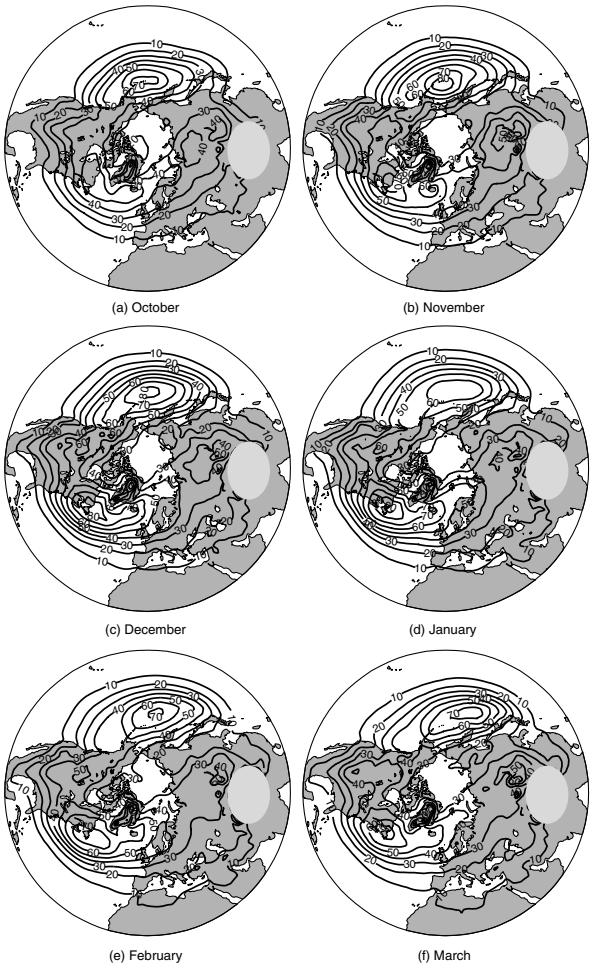

Fig. 1. The long-term mean storminess for (a) October, (b) November, (c) December, (d) January, (e) February and (f) March. Units are in 10^4 $(\text{hPa})^2$.

3. Results

3.1. The seasonal model

The long-term mean storminess for the 6 winter months are shown in Fig. 1. The mid-latitude storm tracks in the North Pacific and North Atlantic can clearly be seen. In the North Pacific the intensity of the storm track has a peak at about 50°N and 170°E. The intensity increases from October through November. In January and February the storm activity reaches a well-known minimum known as the mid-winter suppression of the Pacific storm activity(Nakamura, 1992). The intensity of the North Atlantic storm activity increases from October and reaches a maximum in January. The Pacific storm track can be seen to end rather abruptly in the Rocky mountains while the Atlantic storm track extends further inland over the European and Eurasian continent. Note that the Himalayas have been marked by a lightly shaded region on all the maps. This is done since the reanalysis data have problems extrapolating to SLP due to the large diurnal cycle in the temperature in this region, presumably leading to a lot of spurious high-frequency variability in the SLP field.

The explained variability by the seasonal model, relative to the constant model, is shown in Fig. 2a. In the North Atlantic seasonal variations account for up to 40% of the variability off the east coast of North America. This area coincides with the strong baroclinic zone associated with the surface temperature gradient between the warm Gulf stream and cold continent (Dickson and Namias, 1976). Similarly, in the Pacific seasonality accounts for up to 50% of the variability at the entrance of the storm track. As pointed out by Orlanski (2005) the baroclinicity at the entrance of the Pacific storm track is due to the combination of the land-sea contrast, surface baroclinicity over the ocean and strong moist fluxes from the western subtropics. In the North Pacific the influence of seasonality can be seen to extend further than in the North Atlantic. This is consistent with the zone of large baroclinicity, for instance measured by the Eady growth rate maximum, extending further along the storm track in the North Pacific (Hoskins and Valdes, 1990, fig. 2). Towards the

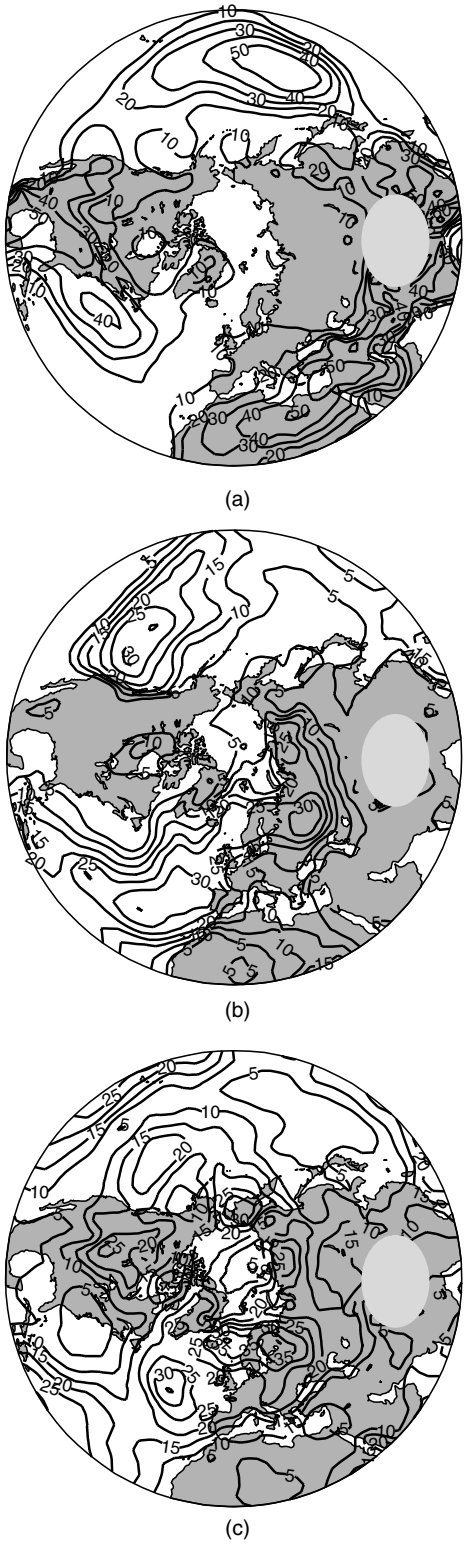

Fig. 2. The explained variability in percentage for the: (a) Seasonal model, (b) Local model and (c) Non-local (teleconnection) model.

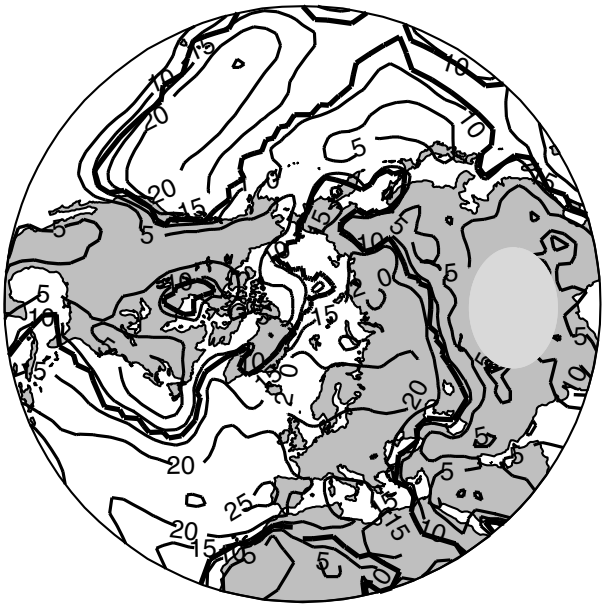

Fig. 3. The percentage change in monthly storminess for an increase of one standard deviation of the local SLP anomaly. Thick black contour marks the areas that are significant at the 5% level.

end of the North Pacific and North Atlantic storm tracks seasonality accounts for less than 20 and 10% of the variability, respectively.

3.2. The local model

Figure 3 shows the percentage change in monthly storminess for an increase of one standard deviation of the local SLP anomaly. The change varies from about −5% at the beginning of both the Atlantic and Pacific storm tracks to −25% at the end. The explained variability of the local model relative to the seasonal model is shown in Fig. 2b. It reaches a maximum of about 30% at the downstream end of both the major storm tracks. In the North Pacific this relationship terminates abruptly when reaching the North American continent and the Rocky mountains. Over the North American continent the local SLP anomaly accounts for less than 5% of the variability. In contrast there is no such clear boundary at the downstream end of the Atlantic storm track. Local SLP account for over 20% of the storminess over Scandinavia, Europe and large parts of Russia.

3.3. The non-local (teleconnection) model

The explained variability of the teleconnection model relative to the seasonal model is shown in Fig. 2c. In the North Pacific the explained variability varies from less than 5% at the entrance to about 20% towards the end. In the North Atlantic the teleconnection patterns explain more of the variability with some areas reaching 35%. The influence of the five

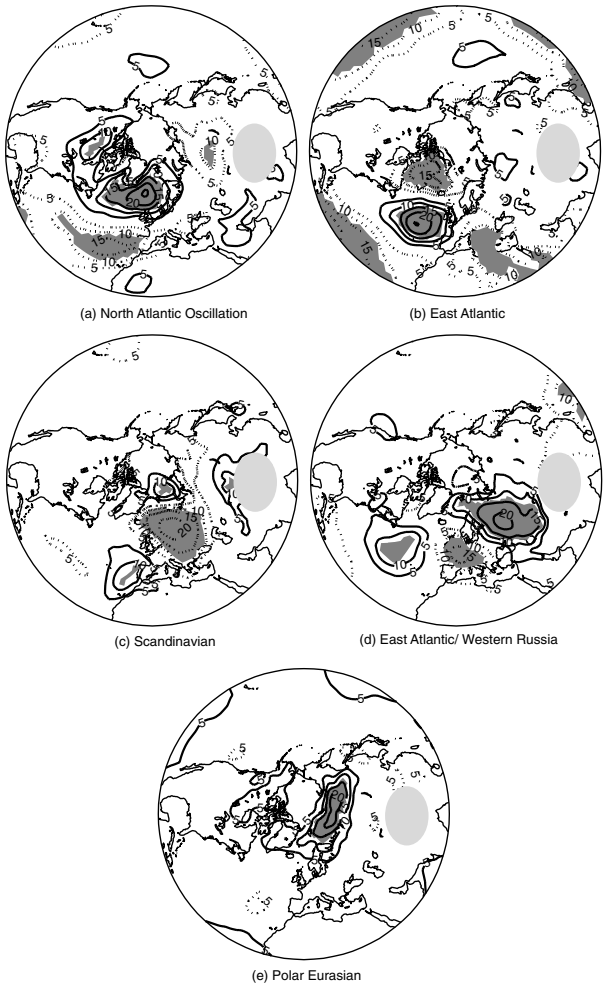

Fig. 4. The percentage change in monthly storminess for an increase of one standard deviation in the teleconnection indices. Dark shaded areas are significant at the 5% level.

leading Euro-Atlantic teleconnections on storminess is shown in Fig. 4. It can be seen that they all have regions that are statistically significant at the 5% level. In Fig. 4a the North Atlantic Oscillation is characterized by the familiar dipole over the Atlantic Ocean as has been well documented in the literature (Hurrell, 1995). Its positive phase is associated with increased storminess in the Icelandic region and decreased storminess further south towards Spain and Portugal. This is consistent with the analysis of Rogers (1990) based on cyclone frequencies and Rogers (1997) using bandpass filtered SLP. However, it is clear that the NAO does not account for all the storminess in the North Atlantic. The East Atlantic pattern is in its positive phase associated with an anomalous low in the North Atlantic at approximately 50–55 degrees North and a higher subtropical high. Figure 4b provides evidence that the East Atlantic pattern is a major factor for Atlantic storminess particularly in the area not accounted for by the NAO. Note also that the East Atlantic pattern accounts for storminess over the Labrador Sea and over a small part of the Mediterranean Sea.

This result may seem to contradict the conclusion by Lau (1988). He found that the East Atlantic pattern was related (correlation of 0.61) to the first eigenvector of Atlantic bandpass filtered 500 hPa geopotential height depicting northward and southward migration of the North Atlantic storm track. The reason for this discrepancy may be partly due to the slightly different definition of the East Atlantic pattern found in Wallace and Gutzler (1981). Another difference is that the leading eigenvector found in Lau (1988) represents only 20% of the variability of monthly storminess while no such truncation is performed in this study.

The Scandinavian Pattern shown in Fig. 4c is another important factor for storminess over Scandinavia and northeastern Europe. It is reminiscent of a wave train and has been linked to tropical convection via Rossby wave propagation (Hoskins and Karoly, 1981). In its positive phase it is often associated with a blocking high over Scandinavia. The storms, therefore, tend to propagate to the north and south of this anomaly (Rex, 1950). It is the pattern with the greatest influence over Scandinavia and western Russia. The East Atlantic/Western Russia pattern in Fig. 4d can be seen to be the dominating factor over Russia and central Europe. The Polar Eurasian pattern,[1] which is associated with the strength of the polar vortex, can be seen in Fig. 4e to be important for storminess over the Barent Sea and northern Russia.

In the North Pacific Fig. 5 shows the PNA pattern to be the most prominent factor. The PNA is comprised of four centres of geopotential height anomalies resembling a wave train originating in the subtropics extending northwards via a great circle route (Hoskins and Karoly, 1981). Its positive phase is associated with a deeper than normal Aleutian low, an extensive ridge over northwestern Canada and a trough over southeastern United States. Lau (1988) found that in particular north-south displacements of the mid-latitude storm track in the eastern Pacific was related to the variability of the PNA pattern. This is consistent with the results shown in Fig. 5a. The PNA can be seen to significantly account for storminess in particular over the eastern North Pacific and slightly north of the Aleutian low. It, therefore, represents a north-south shift of the storm track. The West Pacific pattern is characterized by a dipole in the geopotential height field in the western sector of the North Pacific with negatively correlated centres in the mid-latitude and subtropics. Figure 5b shows that its positive phase leads to increased storminess in the northern part of the Pacific between Kamchatka and Alaska. The East/North Pacific pattern also accounts for some of the storminess in the mid Pacific. Surprisingly, Fig. 5c provides evidence that it accounts for storminess in a small but statistically significant region centred over the Bay of Biscay.

[1] Note that the spatial extent of this pattern was substantially changed in a revision of the CPC teleconnection patterns on 1 July 2005.

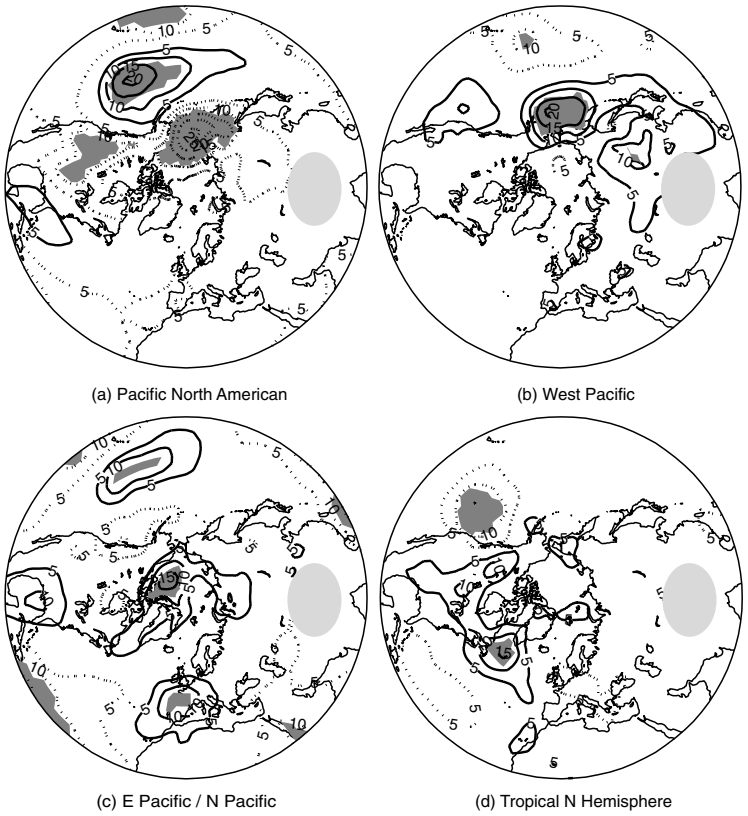

Fig. 5. The percentage change in monthly storminess for an increase of one standard deviation in the teleconnection indices. Dark shaded areas are significant at the 5% level.

3.4. The full model

Figure 6 shows the influence of the teleconnection patterns once seasonality and the local SLP anomaly is accounted for. The North Atlantic Oscillation in Fig. 6b is no longer characterized by a dipole. The storminess over its two centres over the Azores and Iceland is largely accounted for by the local SLP anomaly. However, surprisingly the NAO does provide additional explanation in the mid North Atlantic between the two centres of the dipole and further to the west compared to the teleconnection model in Fig. 4a. To some extent this coincides with the region of the East Atlantic pattern. The reason for this influence of the NAO is not clear. From this study it is only possible to conclude that this signal can only be detected once the effects of the local SLP is removed.

The East Atlantic pattern, as shown in Fig. 6c, does not account for more of the variability of storminess in the Atlantic. The local SLP anomaly is thus an equally good predictor in this area. However, over the Labrador Sea the East Atlantic pattern can be seen to be an important non-local factor for storminess. The Scandinavian Pattern factor in Fig. 6d is similar to the one depicted in Fig. 4c although the statistically significant region over Scandinavia is greatly reduced. Further to the north in the Barents Sea there is a small but significant region. It might reflect increased northerly storminess during blocking highs over Scandinavia associated with positive phases of the Scandinavian Pattern. The East Atlantic/Western Russia pattern factor in Fig. 6e has two significant regions over northern Scandinavia/Russia and the Caspian Sea. Compared to the teleconnection model the pattern no longer has a significant influence in the Atlantic. The influence of the Polar Eurasian factor can be seen in Fig. 6f to have almost disappeared except for a small region over the polar cap.

Figure 7 shows the influence of the Pacific teleconnections once the local SLP anomaly is accounted for. Evidently the PNA pattern is an important non-local factor over western America and outside and over Alaska. However, notably there is no longer a statistically significant region over its southern centre in the North Pacific. In fact none of the teleconnection patterns explain more of the variability of storminess over the North Pacific except for a region far north towards the Bering Strait. Both the West Pacific pattern and the PNA pattern are important non-local factors in this region and are largely unaffected by the local SLP factor. Figure 7c shows the East/North Pacific pattern to only be significant in a small region over the polar cap. The Tropical Northern Hemisphere pattern in Fig. 7d no longer has any statistically significant influence.

3.5. The mean-variance dependency of storminess

The estimated shape parameter ν of the gamma probability distribution is shown in Fig. 8. The shape parameter ν is related to

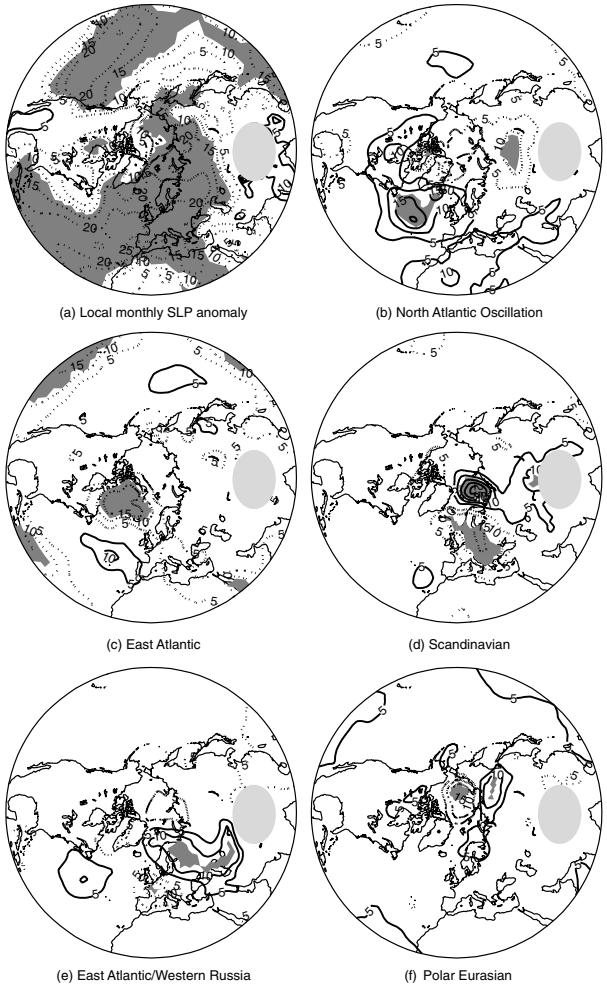

Fig. 6. The percentage change in monthly storminess for an increase of one standard deviation in the predictors. They are based on the full model with both the local SLP anomaly and teleconnection patterns as predictors. Dark shaded areas are significant at the 5% level.

the mean μ and variance σ^2 by:

$$\nu = \left(\frac{\mu}{\sigma}\right)^2. \tag{2}$$

A larger ν implies a more symmetric gamma distribution and less mean-variance dependency (heteroskedasticity). Further details about the estimation of ν can be found in Appendix A1.

There are particularly two interesting features to be seen from the four estimates of the shape parameter in Fig. 8. Firstly, the shape parameter for all models is large at the entrance of the North Pacific and North Atlantic storm tracks and smaller towards the end. In other words there is a greater mean-variance dependency at the end of both storm tracks. A smaller ν implies that the ratio of the mean to the standard deviation is smaller. This may be interpreted in the light of the results of Mailier et al. (2006). By analyzing the relationship between the mean and variance of cyclone counts they found that extratropical cyclones arrive at rather regular intervals at the entrance of the major storm tracks while tending to cluster downstream. The clustering of cyclones thus provides a possible explanation for the greater heteroskedasticity found there. However, by using storminess instead of cyclone counts the heteroskedasticity can also be due to the intensity of cyclones. A few very intense cyclones may have a large effect on the monthly storminess. Secondly, it is evident that ν is increasing as more predictors are added to the model. For instance by comparing the estimates from the seasonal and full model in Figs. 8a and 8b it is clear that ν is larger for the model with all predictors included. Some of the heteroskedasticity is thus accounted for by the teleconnection patterns. This is consistent with the conclusion in Mailier et al. (2006) that teleconnection patterns can account for some of the clustering of extratropical cyclones.

4. Conclusions

Using five gamma regression models this study has aimed to address the following three questions posed in the introduction:

(1) How well can variations in local mean flow account for variations in storminess?

The local SLP anomaly is linearly related to monthly storminess particularly at the downstream end of the extratropical North Pacific and North Atlantic storm tracks. In these regions it represents up to 35% of the variability. At the entrance of both storm tracks it is of little value as a predictor accounting for less than 5% of the variability. Here seasonality is the dominant factor which coincides with regions of large baroclinicity. The increasing influence of the local SLP anomaly along both major storm tracks appears to be consistent with the theory of life cycles for baroclinic waves (Simmons and Hoskins, 1978). In such an idealized view the baroclinic waves are characterized by baroclinic growth at the entrance with increasing fluxes of momentum and heat to larger temporal and spatial scales in its decaying phase. Lau and Nath (1991) have shown that monthly SLP anomalies to a large extent is forced by such synoptic scale vorticity and heat fluxes. The variance of this forcing peaks downstream of the jet stream maxima and may explain why the local model is a better predictor in this area.

(2) Can teleconnection patterns provide additional explanation for variations in storminess?

In the North Pacific the answer is largely no except for the region north of the Aleutian low towards the Bering Strait. In this area the PNA pattern is an important non-local factor for storminess. The southern centre of the PNA, however, simply represents a local relationship between storminess and the SLP anomaly. The reason for this striking difference is not revealed by this study although this result strongly suggests that different dynamical mechanisms are relating storminess to the two centres of the PNA pattern in the North Pacific.

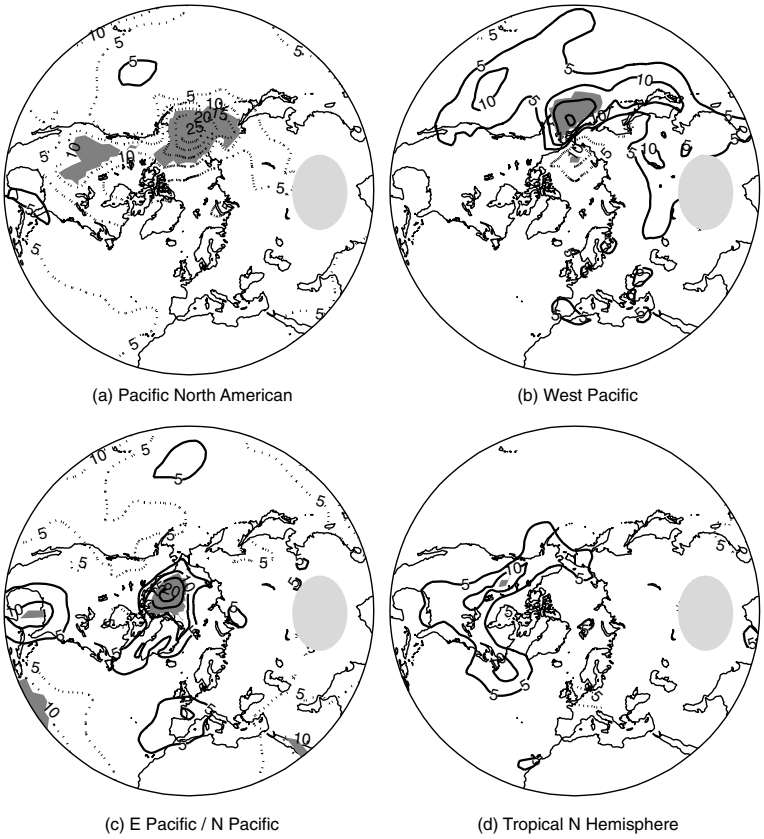

Fig. 7. The percentage change in monthly storminess for an increase of one standard deviation in the predictors. Dark shaded areas are significant at the 5% level. Results are from the full model with both the local SLP anomaly and the teleconnection patterns as predictors

In the North Atlantic the NAO is the only factor that is statistically significant at the 5% level once the local SLP anomaly is accounted for. The NAO in its positive phase accounts for increased storminess in the mid North Atlantic. The East Atlantic pattern is also identified as an important non-local factor for storminess over the Labrador Sea. Over the European continent the Scandinavian pattern and East Atlantic/Western Russia are still significant factors although in a substantially smaller area.

(3) How much of the variability of storminess can be accounted for by the NAO and PNA patterns? Are other teleconnection patterns important for predicting storminess in the Euro-Atlantic region and in the North Pacific?

The results of the teleconnection model show that several teleconnection patterns are important for monthly storminess in the North Atlantic and over Europe. Five teleconnection patterns were found to be significant factors at the 5% level: the NAO, the East Atlantic pattern, the Scandinavian pattern, the East Atlantic/Western Russia pattern and the Polar/Eurasian pattern. In particular the East Atlantic pattern is an important factor for storminess in the middle of the North Atlantic in an area not covered by the NAO dipole. This explains why the East Atlantic pattern rather than the NAO is important for precipitation in the south of England (Murphy and Washington, 2001). In the North Pacific the PNA has been shown to be the dominant factor while the West Pacific pattern and the Tropical Northern Hemisphere pattern only have smaller regions of influence.

This study has also revealed that there is an increasing mean-variance dependency (heteroskedasticity) of storminess along the North Atlantic and North Pacific storm tracks, some of which can be accounted for by the monthly mean flow. This is consistent with the conclusion of the Mailier et al. (2006) study. Based on monthly cyclone counts rather than storminess they showed that extratropical cyclones arrive at regular intervals at the entrance of the major storm tracks while tending to cluster downstream. The possibility of studying the mean-variance dependency of storminess further underlines the usefulness of using GLMs. Due to the flexibility of the Gamma distribution, the GLM models in this study also provide a general linear framework that can easily be used to model storminess on shorter timescales which are likely to be less Gaussian. The likelihood based ratio tests are ideal for detecting relationships in noisy daily data, although then the issue of serial correlation needs to be addressed.

5. Acknowledgments

We would like to thank Matt Sapiano for very useful discussions on GLMs. Richard Chandler is also acknowledged for advice on interpreting residuals in GLMs and for providing some excellent

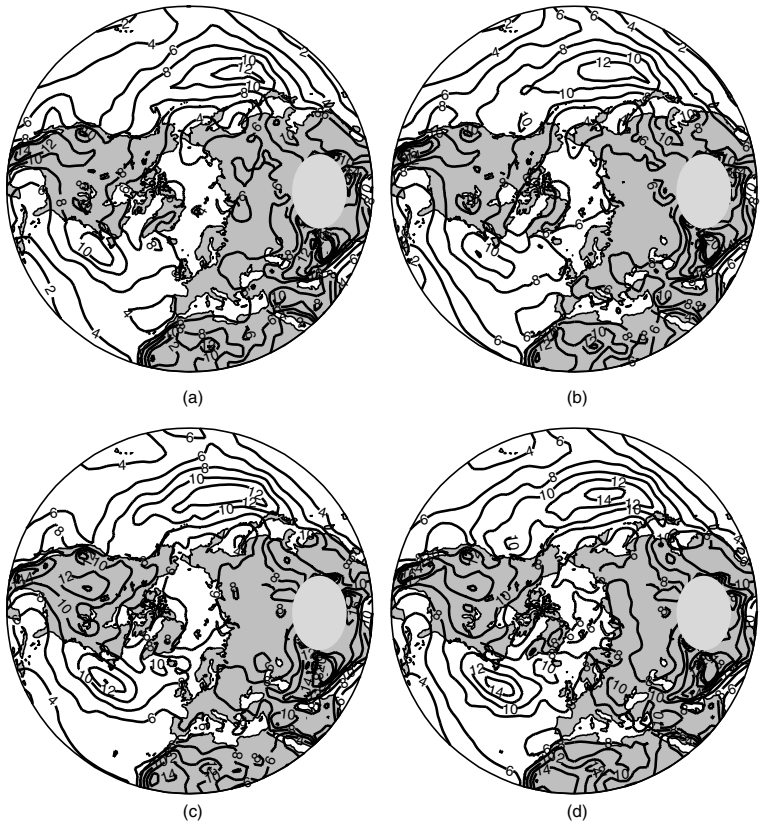

Fig. 8. The estimated shape parameter ν for the conditional Gamma probability distribution: (a) Seasonal model, (b) Local model, (c) Non-local (teleconnection) model and (d) Full model with all predictors included.

lecture notes on GLMs on his website. This work was funded by the Norwegian Research Council under contract 154309/432.

5. Appendix A:

A1. The gamma probability distribution

The gamma probability distribution is defined as:

$$f(y;\mu,\nu) = \frac{1}{y\Gamma(\nu)}\left(\frac{\nu y}{\mu}\right)^{\nu}\exp\left(-\frac{\nu y}{\mu}\right) \quad \nu > 0 \;\; y,\mu \geq 0, \tag{A1}$$

where

$$\Gamma(\nu) = \int_0^\infty t^{\nu-1}e^{-1}dt \;\; \nu > 0. \tag{A2}$$

The parameters of the gamma distribution are the population mean μ and the shape parameter ν. The mean μ is estimated using a maximum likelihood estimator as described in McCullagh and Nelder (1989). The shape parameter ν is estimated using a moment estimator where the inflation caused by fluctuations in μ is removed:

$$\nu^{-1} = \frac{1}{n-p}\sum\left(\frac{y-\hat{\mu}}{\hat{\mu}}\right)^2, \tag{A3}$$

where n is the sample size, p the number of predictors and $\hat{\mu}$ the estimated mean. The shape parameter is in this study assumed constant in time for every grid point. This assumption is checked by fitting a separate model for every winter month (not shown). There is some seasonal variation in the estimated shape parameter along the storm tracks but this variation is small and the assumption appears justified.

To further motivate the use of the Gamma distribution the following example is instructive: Assume that $Z_1, \ldots, Z_n$ are independent standard normal random variables and that $Y = \sum_{i=1}^n Z_i^2$.Y is then gamma distributed: $Y \sim \Gamma(n/2, 1/2)$. This is usually referred to as the chi-squared distribution with n degrees of freedom. This can be written as: $Y = \sum_{i=1}^n Z_i^2 \sim \chi_n^2$. Variance is a sum of squares and so if the highpass filtered SLP was normally distributed and independent from day to day then the monthly variance of highpass filtered SLP would be χ^2 distributed with $n = 30$ degrees of freedom.

A2. Hypothesis testing

The parameters in the GLM models are estimated using maximum likelihood. In order to decide whether a factor significantly influences storminess in a region likelihood ratio tests can then be used. It is based on the idea that significant factors will lead to large increases in the log-likelihood when added to the model. A likelihood ratio test is optimal in the sense that it is the most powerful test for distinguishing between two hypotheses (the Neyman-Pearson lemma).

The following nested-model procedure for likelihood ratio tests is used to determine the significance of predictors: First a model with q predictors is fitted yielding a log-likelihood $\ln L_0$. A new model is then fitted with an additional predictor yielding a log-likelihood $\ln L_1$. A likelihood ratio statistic can then be calculated as:

$$2 \ln \Lambda = 2 \ln \left(\frac{L_1}{L_0} \right). \tag{A4}$$

If Y is gamma distributed then for large samples the test statistic in eq. (A4) is approximately χ^2 distributed with 1 degree of freedom. In order to test whether the added predictor is significant at the 5% level the test statistic must exceed this percentage point for the χ^2 probability distribution with 1 degree of freedom (which is 3.84).

The ratio of log likelihoods can also be used to define the *deviance* which is a useful measure of the goodness of fit of GLM models. It is defined as:

$$D = 2 \ln \left(\frac{L_F}{L_{\text{fitted}}} \right), \tag{A5}$$

where L_F is the likelihood of a perfect model (with as many predictors as observations) and L_{fitted} is the likelihood of the model under consideration. An increase in the likelihood of the fitted model leads to less deviance and, therefore, an improved fit. For the normal distribution the deviance is simply equal to the residual sum of squares (RSS). Analogous to linear regression a "deviance explained" in percentage can be defined as:

$$100 \times \left(\frac{D_{\text{null}} - D_{\text{fitted}}}{D_{\text{null}}} \right), \tag{A6}$$

where D_{null} is the deviance of a reference model and D_{fitted} is the deviance of the fitted model under consideration. Whenever the phrase "explained variability" is used it refers to the explained deviance of the model under consideration relative to a reference model. For the seasonal model the explained variability is relative to a model with just a single constant term. The explained variability of the other models presented here are chosen to be relative to the seasonal model.

References

Barnston, A. G. and Livezey, R. E. 1987. Classification, seasonality and persistence of low-frequency atmospheric circulation patterns. *Mon. Weather Rev.* **115**, 1083–1126.

Blackmon, M. L., Lee, Y. H. and Wallace, J. M. 1984a. Horizontal structure of 500-mb height fluctuations with long, intermediate and short-time scales. *J. Atmos. Sci.* **41**, 961–979.

Blackmon, M. L., Lee, Y. H., Wallace, J. M. and Hsu, H. H. 1984b. Time-variation of 500-mb height fluctuations with long, intermediate and short-time scales as deduced from lag-correlation statistics. *J. Atmos. Sci.* **41**, 981–991.

Chandler, R. 2005. On the use of generalized linear models for interpreting climate variability. *Environmetrics* **16**, 699–715.

Chang, E. K. M. and Fu, Y. F. 2003. Using mean flow change as a proxy to infer interdecadal storm track variability. *J. Climate* **16**, 2178–2196.

Chang, E. K. M., Lee, S. Y. and Swanson, K. L. 2002. Storm track dynamics. *J. Climate* **15**, 2163–2183.

Coe, R. and Stern, R. D. 1982. Fitting models to daily rainfall data. *J. Appl. Meteor.* **21**, 1024–1031.

Dickson, R. R. and Namias, J. 1976. North American influences on the circulation and climate of the North Atlantic sector. *Mon. Weather Rev.* **104**, 1255–1265.

Doblas-Reyes, F. J. and Déqué, M. 1998. A flexible bandpass filter design procedure applied to midlatitude intraseasonal variability. *Mon. Weather Rev.* **126**, 3326–3335.

Elsner, J. B. and Bossak, B. H. 2003. Secular changes to the ENSO-U.S. hurricane relationship. *Geophys. Res. Lett.* **28**, 4123–4126.

Harnik, N. and Chang, E. K. M. 2003. Storm track variations as seen in radiosonde observations and reanalysis data. *J. Climate* **16**, 480–495.

Holton, J. R. 1992. *An Introduction to Dynamic Meteorology*. Academic Press, San Diego, 3rd Edition. pp. 335–342.

Hoskins, B. J. and Hodges, K. I. 2002. New perspectives on the Northern Hemisphere winter storm tracks. *J. Atmos. Sci.* **59**, 1041–1061.

Hoskins, B. J. and Karoly, D. J. 1981. The steady linear response of a spherical atmosphere to thermal and orographic forcing. *J. Atmos. Sci.* **38**, 1179–1196.

Hoskins, B. J. and Valdes, P. J. 1990. On the existence of storm tracks. *J. Atmos. Sci.* **47**, 1854–1864.

Hurrell, J. W. 1995. Decadal trends in the North Atlantic Oscillation and relationships to regional temperature and precipitation. *Science* **269**, 676–679.

Kalnay, E., Kanamitsu, M., Kistler, R., Collins, W., Deaven, D. and co-authors. 1996. The NCEP/NCAR 40-year re-analysis project. *Bull. Amer. Meteorol. Soc.* **77**, 437–471.

Lau, N. C. 1988. Variability of the observed midlatitude storm tracks in relation to low-frequency changes in the circulation pattern. *J. Atmos. Sci.* **45**, 2718–2743.

Lau, N. C. and Holopainen, E. O. 1984. Transient eddy forcing of the time-mean flow as identified by geopotential tendencies. *J. Atmos. Sci.* **41**, 313–328.

Lau, N. C. and Nath, M. J. 1991. Variability of the baroclinic and barotropic transient eddy forcing associated with monthly changes in the midlatitude storm tracks. *J. Atmos. Sci.* **48**, 2589–2613.

Mailier, P. J., Stephenson, D. B., Ferro, C. A. T. and Hodges, K. I. 2006. The serial clustering of extratropical cyclones. *Mon. Weather Rev.* **134**, 2224–2240.

McCullagh, P. and Nelder, J. A. 1989. *Generalized Linear Models* 2nd Edition. Chapman & Hall/CRC, Boca Raton.

Murphy, S. J. and Washington, R. 2001. United Kingdom and Ireland precipitation variability and the North-Atlantic sea-level pressure field. *Int. J. Climatol.* **21**, 939–959.

Nakamura, H. 1992. Midwinter suppression of baroclinic wave activity in the Pacific. *J. Atmos. Sci.* **49**, 1629–1642.

Orlanski, I. 2005. A new look at the Pacific storm track variability: sensitivity to tropical SST's and to upstream seeding. *J. Atmos. Sci.* **62**, 1367–1390.

Paciorek, C. J., Risbey, J. S., Ventura, V. and Rosen, R. D. 2002. Multiple indices of Northern Hemisphere cyclone activity, winters 1949–1999. *J. Climate* **15**, 1573–1590.

Panagiotopoulos, F., Shahgedanova, M. and Stephenson, D. B. 2002. A review of Northern Hemisphere winter-time teleconnection patterns. *J. Phys. IV* **12**, 27–47.

Pettersen, S., 1956. *Weather Analysis and Forecasting*, Volume **1**, McGraw-Hill.

Quadrelli, R. and Wallace, J. M. 2004. A simplified linear framework for interpreting patterns of Northern Hemisphere wintertime climate variability. *J. Climate* **17**, 3728–3744.

Rex, D. 1950. Blocking action in the middle troposphere and its effect upon regional climate. *Tellus* **2**, 196–211.

Rogers, J. C. 1990. Patterns of low-frequency monthly sea-level pressure variability (1899–1986) and associated wave cyclone frequencies. *J. Climate* **3**, 1364–1379.

Rogers, J. C. 1997. North Atlantic storm track variability and its association to the North Atlantic Oscillation and climate variability of northern Europe. *J. Climate* **10**, 1635–1647.

Sapiano, M. R. P., Stephenson, D. B., Grubb, H. J. and Arkin, P. A. 2006. Diagnosis of variability and trends in a global precipitation dataset using a physically motivated statistical model. *J. Climate* **19,** 4154–4166.

Simmons, A. and Hoskins, B. 1978. The life-cycles of some non-linear baroclinic waves. *J. Atmos. Sci.* **35**, 414–432.

Trenberth, K. E., Branstator, W. G., Karoly, D., Kumar, A., Lau, N. C. and co-authors. 1998. Progress during TOGA in understanding and modelling global teleconnections associated with tropical sea surface temperatures. *J. Geophys. Res.* **103**, 14 291–14 324.

Vallis, G. K., Gerber, E., Kushner, P. J. and Cash, B. A. 2004. A mechanism and simple dynamical model of the North Atlantic Oscillation and annular modes. *J. Atmos. Sci.* **61**, 264–280.

Wallace, J. M. and Gutzler, D. S. 1981. Teleconnections in the geopotential height field during the Northern Hemisphere winter. *Mon. Weather Rev.* **109**, 784–812.

Wallace, J. M., Lim, G. H. and Blackmon, M. L. 1988. On the relationship between cyclone tracks, anticyclone tracks and baroclinic wave guides. *J. Atmos. Sci.* **45**, 439–462.

Whitaker, J. S. and Sardeshmukh, P. D. 1998. A linear theory of extratropical synoptic eddy statistics. *J. Atmos. Sci.* **55**, 237–258.

Yan, Z., Bate, S., Chandler, R. E., Isham, V. and Wheater, H. 2002. An analysis of daily maximum wind speed in northwestern Europe using generalized linear models. *J. Climate* **15**, 2073–2088.